Mol. Cryst. Liq. Cryst., Vol. 530: pp. 137/[293]–143/[299], 2010

ISSN: 1542-1406 print/1563-5287 online
DOI: 10.1080/15421406.2010.499301

Taylor & Francis
Taylor & Francis Group

Luminence Efficiency and Color Stabilization of Blue Organic Light-Emitting Devices Fabricated Utilizing a 4,7-diphenyl-1,10-phenanthroline Electron Transport Layer Containing an Ultra Thin Trap Layer

DONG CHUL CHOO,[1] KWANG SEOP LEE,[1]
TAE WHAN KIM,[1] JI HYUN SEO,[2]
JEONG HYUN PARK,[2] AND YOUNG KWAN KIM[2]

[1]Advanced Semiconductor Research Center, Department of Electronics and Communications Engineering, Hanyang University, Seoul, Korea
[2]Department of Information Display Engineering & COMID, Hong-ik University, Seoul, Korea

The hole blocking barrier in organic light-emitting devices (OLEDs) fabricated utilizing a 4,7-diphenyl-1,10-phenanthroline (BPhen) electron transport layer (ETL) with an ultra thin trapping layer was affected by the 5,6,11,12-tetraphenylnaphthacene (rubrene) or the tris(8-hydroxyquinoline) (Alq_3) trapping layer, acting as a trapping layer in the ETL. While the rubrene layer in the ETL decreased the number of electrons and holes in the emitting layer (EML), resulting in a decrease in the current density and the luminence of the OLEDs, the Alq_3 layer in the BPhen ETL did not block effectively the holes transfer from the EML to the ETL, resulting in a decrease in the luminence efficiency. The electroluminescence spectra showed that the magnitude of the holes blocked by the ETL was not significantly affected by the thin rubrene layer embedded in the BPhen ETL.

Keywords Color stabilization; luminence efficiency; optical properties; organic light-emitting devices

I. Introduction

Organic light-emitting devices (OLEDs) have emerged as promising candidates for potential applications in the fabrications of full-color flat-panel displays with a large area [1–3]. OLEDs have become particularly interesting due to their unique advantages of low driving voltage, low power consumption, high contrast ratio, wide viewing angle, low production cost, and fast response time [4–6]. Moderate controls

Address correspondence to Prof. Tae Whan Kim, Department of Electronics and Communications Engineering, Hanyang University, 17 Haengdang-dong, Seongdong-gu, Seoul 133-791, Korea (ROK). Tel.: (+82) 2-2220-0354; Fax: (+82) 2-2292-4135; E-mail: twk@hanyang.ac.kr

of carrier injection and transport for efficient carrier recombination and balance of the electrons and the holes are very important for fabricating high-efficiency OLEDs [7,8], Among the various methods for improving the balance of electrons and holes in the emitting layer (EML) for highly efficient OLEDs [9–12], OLEDs utilizing a 4,7-diphenyl-l,10-phenanthroline (BPhen) layer, acting as a hole blocking layer or an electron transport layer (ETL), have been fabricated to improve their efficiencies [13]. However, the lifetime of OLEDs with a BPhen layer is relatively short due to the poor material stability of the BPhen layer. Because the material stability of a BPhen layer used in the OLEDs is related to the remaining time of holes in BPhen molecules [14], studies concerning the hole blocking variation in blue OLEDs utilizing the BPhen layer with an ultra thin trap layer arc still necessary for enhancing device performance.

This paper reports data for a hole blocking variation in blue OLEDs resulting from the existence of an ultra thin trap layer embedded into a BPhen ETL. Current density-voltage, luminence-voltage, luminence efficiency-current density, Commission Internationale de l'éclairage (CIE) coordinates, and electroluminescence (EL) measurements were carried out to investigate the electrical and optical properties of OLEDs utilizing a BPhen ETL with an ultra thin layer. The variations of the luminence efficiency and the color stability dependent on the current density of the OLEDs are described on the basis of the experimental results.

II. Experimental Details

Indium-tin-oxide (ITO) thin films with a sheet resistivity of 20 Ω/square coated on glasses were used as the substrates in this study. The ITO-coated glass substrates were cleaned by using acetone and methanol at 60°C for 5 min and thoroughly rinsed in de-ionized water. The chemically cleaned ITO-coated glass substrates were then dried by using N_2 gas with a purity of 99.9999%, and the surface of the substrates was treated with oxygen plasma for 10 min at an O_2 pressure of approximately 2×10^{-2} Torr. The three kinds of samples used in this study were deposited on ITO-coated glass substrates by using an organic molecular beam deposition with tungsten effusion cells and shutters. The schematic energy band diagrams for the OLEDs of devices I, II, and III are shown in Figure 1. The 5,6,11,12-tetraphenylnaphthacene (rubrene) layer inserted into the EML was attributed to the position of the recombination zone. The hole blocking barrier was affected by the rubrene or the tris(8-hydroxyquinoline) (Alq_3) trapping layer near the left edge of the BPhen ETL. Because the electron mobility in the BPhen layer at 1×10^5 V/cm is approximately 10^{-4} cm^2/Vs and the highest occupied molecular orbital (HOMO) level of the BPhen layer is −6.4 eV, the BPhen layer in the OLEDs is used as an ETL or a hole blocking layer [15]. The HOMO level of the ultra thin layer in devices II and III is higher than that of the BPhen layer, resulting in a decrease in the hole blocking barrier. The ultra thin layers of devices II and III are an Alq_3 layer and a rubrene layer, respectively. While the lowest unoccupied molecular orbital (LUMO) levels of the Alq_3 and the rubrene layers are almost the same, the HOMO level of the rubrene is larger by 0.44 eV than that of the Alq_3 layer. The distance between the right edge of the EML and the ultra thin trapping layer is 5 nm and the width of the ultra thin trapping layer is 2 nm. The depositions of the OLED layers were done at a substrate temperature of 27°C and a system pressure of 5×10^{-8} Torr. The growth rates of the organic layers and the metal layers were approximately 1 and

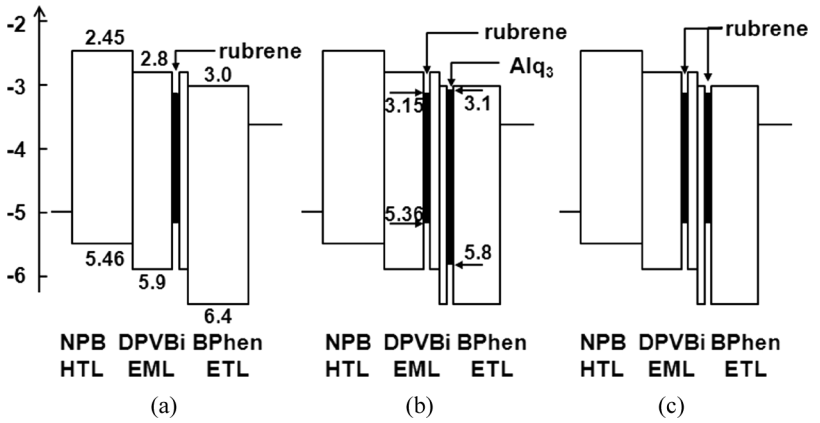

Figure 1. Schematic energy band diagrams for devices (a) I, (b) II, and (c) III.

10 Å/s, respectively, which were controlled by using a quartz crystal thickness monitor. After organic and metal depositions, the OLEDs were encapsulated in a glove box with O_2 and H_2O concentrations below 1 ppm. A desiccant material consisting of barium-oxide powder was used to absorb the residue moisture and oxygen in the encapsulated device. The size of the emitting area in the pixel was $3 \times 3\,mm^2$. All measurements were conducted at room temperature in an ambient environment. The current density-voltage characteristics of the OLEDs were measured on a programmable electrometer with built-in current and voltage measurement units (model 236, Keithely). The brightness was measured by using a brightness meter, chroma meter CS-100A (Minolta), and the EL spectra were obtained using a LS50B (Perkin Elmer) EL spectrometer.

III. Results and Discussion

Figure 2 shows the (a) current density-voltage, (b) luminence-voltage, and (c) luminence efficiency-current density characteristics for the OLEDs of devices I, II, and III. While the current density of device II with an Alq_3 layer inserted into the BPhen ETL is slightly larger than that of device I with a pure BPhen ETL, that of device III with a rubrene layer inserted into the BPhen ETL significantly decreases. The difference of the LUMO levels of the rubrene layer and the Alq_3 layer is very small, and the thicknesses of these layers are too small to affect the electron transport in the ETL. The difference in the current densities for devices II and III dominantly originates from the energy difference in the HOMO levels of the Alq_3 layer and the rubrene layer. Because the HOMO level of the Alq_3 layer in device II is almost the same value as that of the DPVBi EML, the more holes in the EML inject into the ETL due to a decrease in the hole blocking barrier of the ETL in device II. However, because the HOMO level of the rubrene layer is higher than that of the Alq_3 layer, the rubrene layer acts as a hole trap site, resulting in an increase of the trapped holes in the rubrene layer. While the current density of device II is larger than those of other devices, the luminence of device I is larger than that of device II because the Alq_3 layer in device II decreases the hole blocking barrier of the BPhen ETL. The luminence efficiency for the OLEDs of device III with the rubrene layer inserted into the BPhen ETL is slightly higher than those of devices I and II. The rubrene layer in

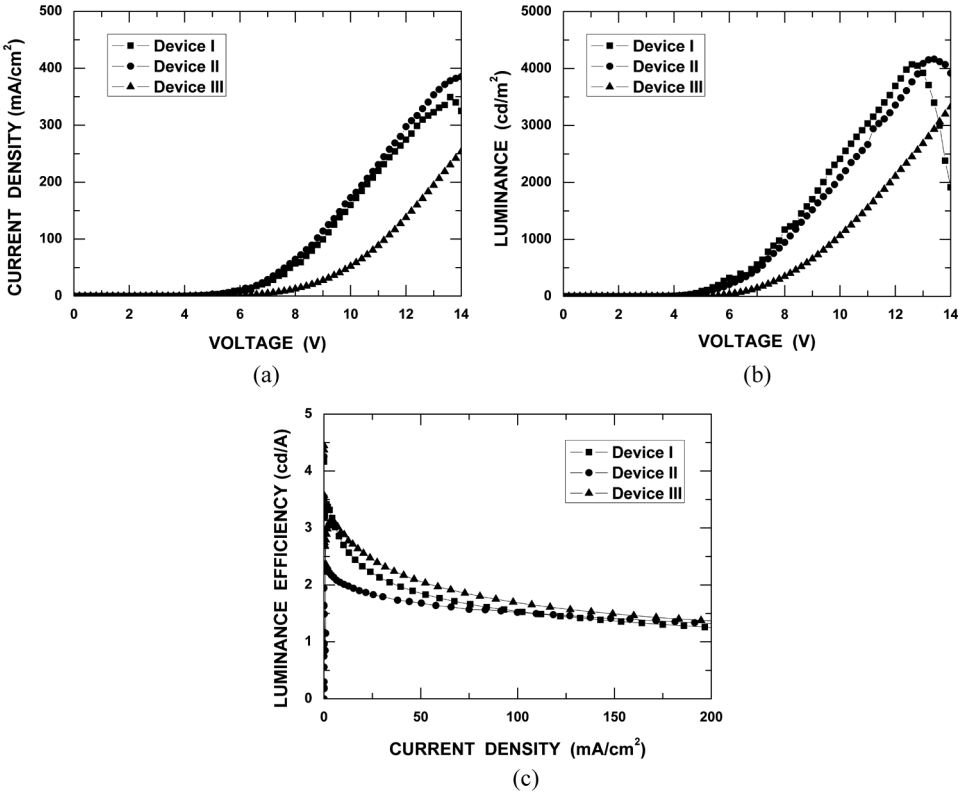

Figure 2. (a) Current densities as functions of the applied voltage, (b) luminances as functions of the applied voltage, and (c) luminance efficiencies as functions of the current density for devices I, II, and III. Filled rectangles, circles, and triangles represent devices I, II, and III, respectively.

the BPhen ETL for device III decreases the hole injection from the EML to the ETL, resulting in an increase in the luminence efficiency of device III.

Figure 3 shows the EL spectra for OLEDs of devices I, II, and III. The EL peaks of 450 and 555 nm correspond to the DPVBi EML and the rubrene layer, respectively. The rubrene peak intensity of device I with a pure BPhen ETL increases with increasing applied voltage up to 6 V but decreases above 6 V. An increase in the rubrene peak is related to the increase in the holes blocked by the BPhen ETL. The peak intensity corresponding to the rubrene layer for device II with the Alq_3 layer inserted into the BPhen ETL is the lowest value among all the devices resulting from a decrease in the holes blocked by the BPhen ETL with an Alq_3 layer. The rubrene peak intensity for device III increases with increasing applied voltage up to 8 V but decreases above 8 V. Even though the number of the rubrene layers of device III is larger than that of device I, the peak intensity related to the rubrene layer of device III is smaller than that of device I. Because the rubrene layer in the BPhen ETL does not contribute to the emission process, the BPhen ETL with a rubrene layer moves the recombination zone of electrons and holes to the center of the EML, resulting in a decrease in the EL intensity.

Figure 4 shows the CIE color coordinates for the OLEDs of devices I, II, and III. The CIE coordinates vary with changes in the applyed voltage due to the shift

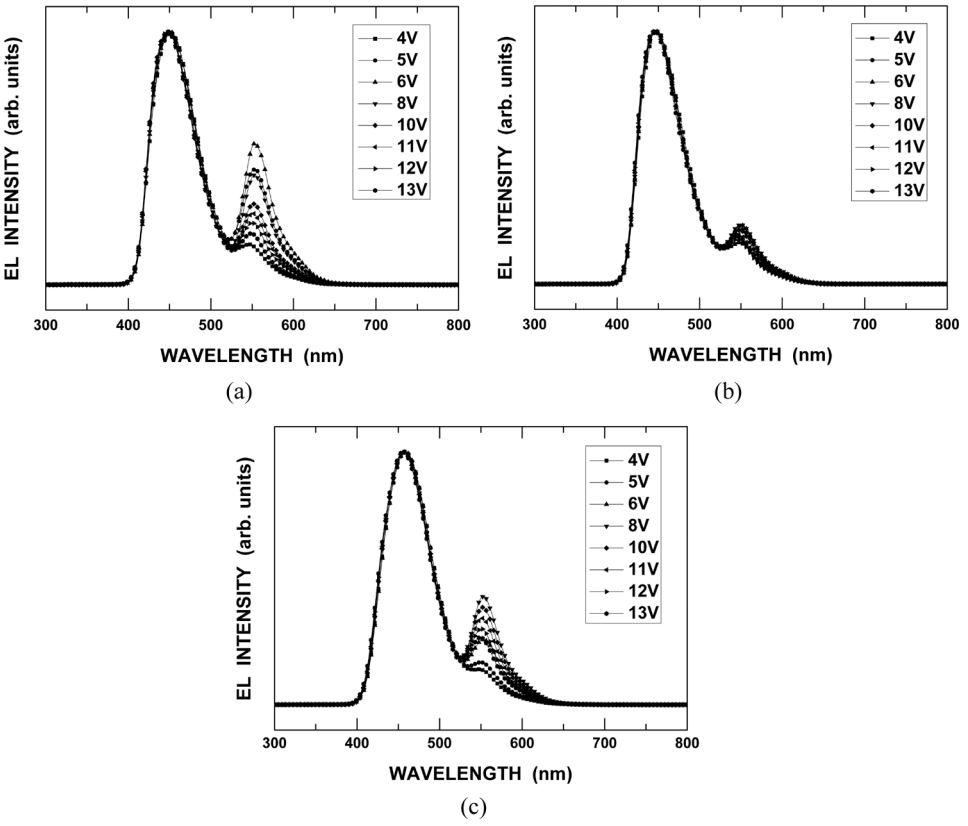

Figure 3. Electroluminescence spectra at several applied voltages for devices (a) I, (b) II, and (c) III.

of the recombination zone. The recombination zone in the EML moves from the left edge of the EML toward its right edge due to an increase in the holes of the EML resulting from the increase of the applied voltage. The pure BPhen layer in device I blocks the transport of the holes and the diffusion of the excitons from the EML to the ETL, resulting in an increase in the holes and the excitons existing in the right side of the EML. Therefore, the rubrene peak intensity in device I is significantly affected by increasing the applied voltage. The rubrene peak with a very small intensity of device II is not significantly affected by increasing the applied voltage due to an increase in the number of holes injected to the ETL resulting from the existence of the Alq_3 layer. Because the HOMO level of the Alq_3 layer in the BPhen ETL is almost the same value as that of the DPVBi EML, the holes inject into the ETL and recombine the electrons in the ETL, resulting in the vanishment of the exciton energy through the non-radiative process because the position of the exciton generation is very close to the cathode electrode. While the luminence efficiency for device II is the lowest value due to the exciton quenching, the color coordinates are the most stable. Because the transport of holes in device II is not disturbed due to the existence of the trapping layer or the hole blocking layer, the recombination zone is not affected by increasing the applied voltage.

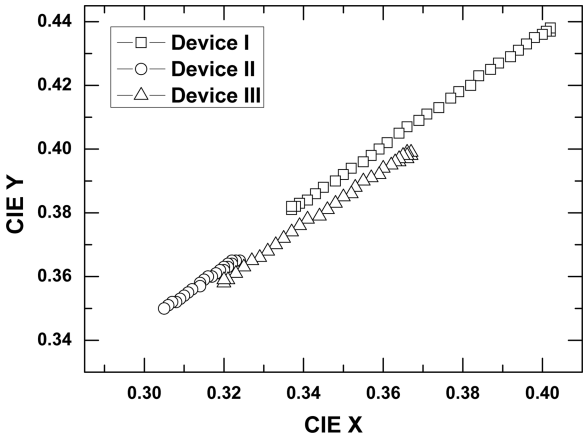

Figure 4. Commission Internationale de l'éclairage coordinates for devices I, II, and III. The color coordinates were plotted in the applied voltage range between 6 and 13 V. Open rectangles, circles, and triangles represent devices I, II, and III, respectively.

IV. Summary and Conclusions

The hole blocking variation in blue OLEDs due to the existence of an ultra thin trap layer embedded into a BPhen ETL was investigated. The ultra thin rubrene or Alq_3 layer inserted into the BPhen ETL of the OLEDs varied the hole blocking barrier of the BPhen ETL. The HOMO level of the rubrene layer was different from that of the DPVBi EML and increased the hole blocking effect due to the holes being trapped in the rubrene layer. This results in a shift of the recombination zone in the EML to the ETL. The Alq_3 layer in the BPhen ETL increased the hole penetration into the ETL due to the almost identical value of the LUMO levels of the DPVBi EML and the Alq_3 layer, causing a decrease in the luminence efficiency of the OLEDs. While the Alq_3 layer did not change the position of the recombination zone in the EML, the stability of the color coordinates for the OLEDs was improved by the existence of the Alq_3 layer. These results can help improve understanding of the hole blocking variation in blue OLEDs caused by the existence of an ultra thin trap layer embedded into a BPhen ETL.

Acknowledgments

This work was supported by the National Research Foundation of Korea (NRF) grant funded by the Korea government (MEST) (No. 2010-0018877).

References

[1] Sun, Y., Giebink, N. C., Kanno, H., Ma, B., Thompson, M. E., & Forrest, S. R. (2006). *Nature*, *440*, 908.
[2] Segal, M., Singh, M., Rivoire, K., Difley, S., Voorhis, T. V., & Baldo, M. A. (2007). *Nature Mater.*, *6*, 374.
[3] Gather, M. C., Köhnen, A., Falcou, A., Becker, H., & Meerholz, K. (2007). *Adv. Funct. Mater.*, *17*, 191.
[4] Young, R. H., Tang, C. W., & Marchetti, A. P. (2002). *Appl. Phys. Lett.*, *80*, 874.

[5] Liew, Y.-F., Zhu, F., Chua, S.-J., & Tang, J. X. (2004). *Appl Phys. Lett.*, *85*, 4511.
[6] Okumoto, K., Kanno, H., Hamada, Y., Takahashi, H., & Shibata, K. (2006). *Appl. Phys. Lett.*, *89*, 013502.
[7] Choo, D. C., Bang, H. S., Kwack, B. C., Kim, T. W., Kim, J. H., Seo, J. H., & Kim, Y. K. (2008). *Thin Solid Films*, *516*, 3610.
[8] Yoon, Y. B., Choo, D. C., Kim, T. W., Lee, H. K., Kim, J. H., & Kim, Y. K. (2007). *Jpn. J. Appl. Phys.*, *46*, 654.
[9] Lee, J.-H., Wu, M.-H., Chao, C.-C., Chen, H.-L., &. Leung, M.-K. (2005). *Chem. Phys. Lett.*, *416*, 234.
[10] Liao, L. S., Slusarek, W. K., Hatwar, T. K., Ricks, M. L., & Comfort, D. L. (2007). *Adv. Mater.*, *20*, 324.
[11] Pfeiffer, M., Leo, K., Zhou, X., Huang, J. S., Hofmann, M., Werner, A., & Blochwitz, J. (2003). *Org. Electron.*, *4*, 89.
[12] Choy, W. C. H., Hui, K. N., Fong, H. H., Liang, Y. J., & Cliui, P. C. (2006). *Thin Solid Films*, *509*, 193.
[13] Naka, S., Okada, H., & Onnagawa, H. (2000). *Appl. Phys. Lett.*, *76*, 197.
[14] Han, S., Wang, L., Lei, G., & Qiu, Y. (2005). *Jpn. J. Appl Phys.*, *44*, L1 82.
[15] Gebyehu, D., Waizer, K., He, G., Pfeiffer, M., Leo, K., Brandt, J., Gerhard, A., Stöβel, P., & Vestweber, H. (2005). *Synth. Metal.*, *148*, 205.